Development of a Dual Isotope Co-Magnetometer Using Laser Cooled Rubidium Toward Electron Electric Dipole Moment Measurement Using Francium

IOP Conf. Series: Journal of Physics: Conf. Series **1206** (2019) 012008 doi:10.1088/1742-6596/1206/1/012008

Development of a Dual Isotope Co-Magnetometer Using Laser Cooled Rubidium Toward Electron Electric Dipole Moment Measurement Using Francium

A Uchiyama[1] , K Harada[1] , T Inoue[2,3] , H Kawamura[1,4] , K S Tanaka[1] , M Itoh[1] , T Aoki[5] , A Hatakeyama[6] , Y Takahashi[7] and Y Sakemi[8]

[1] Cyclotron and Radioisotope Center, Tohoku University, Aoba 6-3, Aramaki, Aoba-ku, Sendai, Japan. Contact Phone: +81227957796
[2] Nishina Center for Accelerator-Based Science, RIKEN, Wako, Japan
[3] Cluster for Pioneering Research, RIKEN, Wako, Japan
[4] Frontier Research Institute for Interdisciplinary Sciences, Tohoku University, Sendai, Japan
[5] Graduate School of Arts and Sciences, University of Tokyo, Tokyo, Japan
[6] Department of Applied Physics, Tokyo University of Agriculture and Technology, Tokyo, Japan
[7] Department of Physics, Kyoto University, Kyoto, Japan
[8] Center for Nuclear Study, University of Tokyo, Tokyo, Japan

E-mail: uchiyama@cyric.tohoku.ac.jp

Abstract. We have developed a dual-rubidium-isotope magneto-optical tap (MOT) for a dual species co-magnetometer used in measurements of the electron electric dipole moment (EDM) using laser-cooled francium atoms. The EDM measurement using atoms in an optical dipole force trap exhibits the advantage of less Doppler effects and longer interaction time compared to atomic and molecular beam experiments. In EDM experiments, the fluctuation of the magnetic field and the vector light shift induced by an optical dipole force can cause systematic errors. The dual species co-magnetometer is being developed to simultaneously monitor the fluctuations of both the magnetic field and the vector light shift. We demonstrated the dual-rubidium-isotope MOT for the development of the dual species co-magnetometer.

1. Introduction

The search for the electric dipole moment (EDM) of elementary particles has been ongoing for more than half a century [1]. In the standard model, the magnitude of an electron EDM is predicted to be $|d_e| < 10^{-38}\,e$cm [2], which is small, because the EDM directly violates the time reversal symmetry [3]. The EDM can verify physics beyond the standard models which predict larger EDM values [3].

The electron EDM has been searched by measuring the energy split of atoms and molecules in an electric field [4, 6, 5]. Francium (Fr) atom is the heaviest alkali atom and exhibits large enhancement factor for the electron EDM compared to other atoms [8, 9]. We conduct the electron EDM search using Fr atoms trapped in an optical dipole force trap [10, 11, 12]. The Fr are produced by the nuclear fusion reaction between an accelerated oxygen beam (100 MeV

$^{18}O^{5+}$) and a fixed gold target. The produced Fr are extracted by an electric field as an ion beam and converted to neutral atoms on an yttrium (Y) foil [13]. After the Fr ions are accumulated on the Y surface, the surface of the Y foil is turned to the direction of a glass cell. Octadecyltrichlorosilane was used to coat the inner walls of the glass cell to prevent the adsorption of atoms on the surface of the glass [14]. The neutralized Fr atoms are released from the Y foil by heating the Y foil. We performed the magneto-optical trapping (MOT) of Fr.

In the EDM measurement using Fr atoms, we measure two atomic resonance frequencies that is in the electric field parallel to the magnetic field, and the electric field anti-parallel to the magnetic field in the ODT. The frequency difference is determined by the interaction between the electric field and the permanent atomic EDM. The fluctuation of the Zeeman shift and the vector light shift (VLS) caused by the ODT can lead to systematic errors. The fluctuation of the VLS result from the fluctuation of the power and the polarization of the light used for the ODT. We are developing the dual species co-magnetometer for evaluating the fluctuation of the frequency shift caused by the Zeeman shift and VLS.

The dual species MOT is the first step toward realizing the dual species co-magnetometer using atoms in the ODT. We studied dual-rubidium (Rb)-isotope MOT using a single external cavity diode laser (ECDL) and an electro-optic modulator (EOM) [15]. In this study, the dual-Rb-isotope MOT system was developed into the system using two ECDLs and EOMs. For loading the atoms to the ODT, the atoms should be sufficiently cooled. The temperature of atoms can be estimated by the time evolution of the radius of the atomic cloud. In this paper, we report the status of the development of the dual-Rb-isotope co-magnetometer, especially on the absorption imaging of each isotope in the dual-Rb-isotope MOT.

2. Experiments

Our experimental setup is shown in Fig. 1. Four different frequencies of lights were required for the dual-Rb-isotope MOT. Two external cavity diode lasers (ECDL-1 and ECDL-2) were used as light sources [Fig. 1 (a)]. The light for trapping ^{85}Rb and ^{87}Rb was generated using ECDL-1 and an electro-optic modulator (EOM-1). The frequency difference between the transition of $5S_{1/2}$, $F = 3 \rightarrow F' = 4$ in ^{85}Rb and the transition of $5S_{1/2}$, $F = 2 \rightarrow F' = 3$ in ^{87}Rb was 1126 MHz. The frequency of ECDL-1 was stabilized to the resonant frequency of the transition of $5S_{1/2}$, $F = 3 \rightarrow F' = 4$ in ^{85}Rb with detuning frequency of -200 MHz. The RF signal with frequency of 1126 MHz was input to EOM-1 for the generation of sidebands. The light for repumping ^{85}Rb and ^{87}Rb from the state of $5S_{1/2}$, $F = 2$ in ^{85}Rb and $5S_{1/2}$, $F = 1$ in ^{87}Rb was generated using ECDL-2 and EOM-2. The frequency difference between the transition $5S_{1/2}$, $F = 2 \rightarrow F' = 3$ in ^{85}Rb and the transition $5S_{1/2}$, $F = 1 \rightarrow F' = 2$ in ^{87}Rb was 2527 MHz. The frequency of ECDL-2 was stabilized to the resonant frequency of the transition $5S_{1/2}$, $F = 1 \rightarrow F' = 2$ in ^{87}Rb with detuning frequency -180 MHz. The RF signal with frequency of 2527 MHz was input to EOM-2 for generation of sidebands. The powers of the laser beams with sidebands were amplified by the tapered amplifiers. The frequencies of the lights for trapping and repumping were shifted by +180 MHz respectively using acousto-optic modulators (AOMs).

First, Rb atoms from a Rb ample were cooled and trapped in MOT-1. A pushing beam was used to transfer cooled atoms from MOT-1 to MOT-2 (right chamber shown in Fig. 1 (c)) region where the co-magnetometer experiment are planed to be conducted. The pushing beam was generated from ECDL-1 and +200 MHz frequency-shifted using an AOM. The typical vacuum pressure in MOT-1 was 3×10^{-8} Pa, and that in MOT-2 was 5×10^{-10} Pa. Coils in quadrupole configuration produced the magnetic field gradient of 10 G/cm and 22 G/cm in the vicinity of center in MOT-1 and MOT-2, respectively.

To estimate the temperature and number of trapped atoms, the atomic cloud distribution in MOT-2 was observed. The absorptive shadow formed by the cloud in the probe beam was

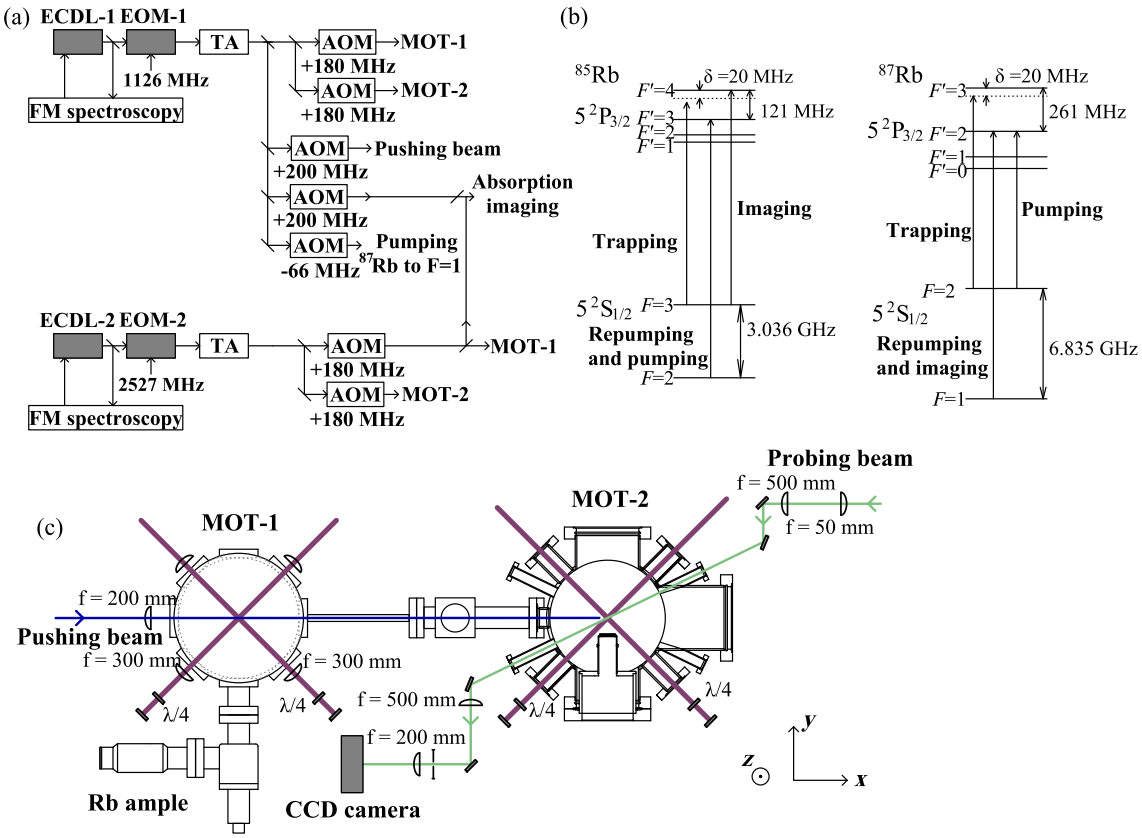

Figure 1. Experimental setup. (a) Schematic diagram of the optical system used in this experiment. (b) Schematic energy diagrams of ^{85}Rb and ^{87}Rb. (c) Layout of MOT-1 and MOT-2. The laser beams in the z-axis are not illustrated here but they were used in both MOT-1 and MOT-2.

imaged onto a charge-coupled-device (CCD) camera. The timing sequence of the absorption imaging is shown in Fig. 2. For imaging the ^{85}Rb atoms, atoms were pumped to the state of $5S_{1/2}$, $F = 3$ using a laser beam, which was used for repumping during the MOT. The ^{85}Rb atoms pumped to the state of $5S_{1/2}$, $F = 3$ were probed with light that was generated from ECDL-1 and frequency shifted by +200 MHz using an AOM. When the absorption imaging of ^{85}Rb was performed, the 1126-MHz signal was not input to EOM-1. For imaging the ^{87}Rb atoms, atoms were pumped to the the state of $5S_{1/2}$, $F = 1$ using the laser beam that was generated from ECDL-1 shifted by -66 MHz using an AOM. The frequency of the ^{87}Rb pumping beam was the resonance frequency of the transition $5S_{1/2}$, $F = 2 \rightarrow F' = 2$ in ^{87}Rb. The ^{87}Rb atoms pumped to the state of $5S_{1/2}$, $F = 1$ were probed with light that was the same frequency as that of the light used for repumping ^{87}Rb to $F = 2$. When the^{87}Rb atoms were probed, the RF signal with frequency of 2527 MHz was not input to EOM-2.

3. Results and Discussions

We observed the absorption image of ^{85}Rb and ^{87}Rb atoms trapped in the dual-Rb-isotope MOT. The input powers of the 1126-MHz and 2527-MHz signals to EOM-1 and EOM-2 were 17 dBm and 20 dBm, respectively. The carrier and first-order sideband intensities of the light from EOM-1 and EOM-2 were approximately 25% and 32 %, respectively. The laser power including all of the frequencies for trapping were 20 mW and 14 mW along each axis of MOT-1

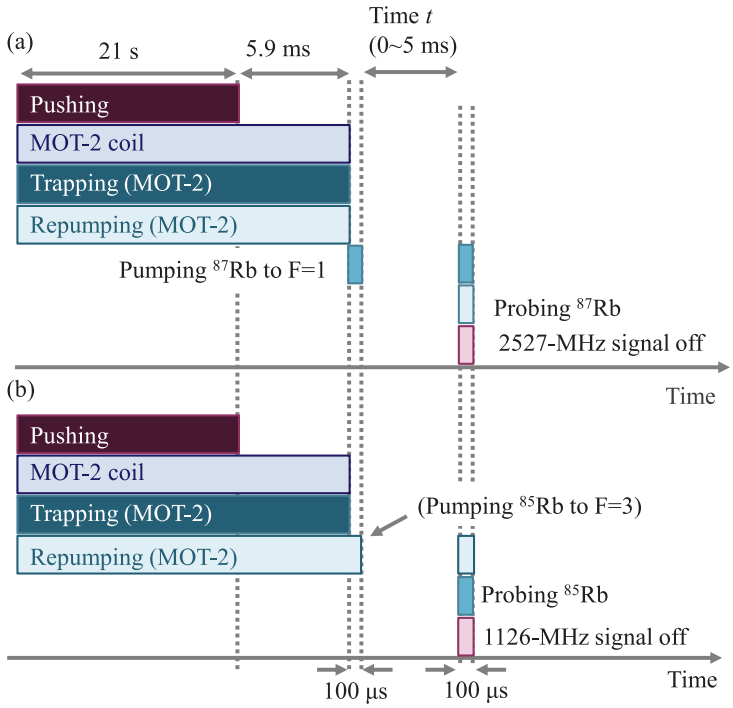

Figure 2. Time sequence of imaging (a)^{87}Rb and (b)^{85}Rb atoms. Atoms were loaded from MOT-1 to MOT-2 using the pushing beam for 21 s. The coils for MOT-2 and the light for trapping and repumping maintain for 5.9 ms after the pushing beam was stopped. Atoms were pumped to one hyperfine state in 100 μs and probed after a certain delay time t. When the atoms were probed, the input signals for the EOMs were turned off to extinguish sidebands.

and MOT-2, respectively. The combined laser power for repumping was 9 mW for the z-axis of MOT-1 and 2 mW for each axis of MOT-2. The laser power for the pushing beam from MOT-1 to MOT-2 was 1.3 mW. The laser power for optical pumping ^{87}Rb atoms to the state $F = 1$ was 0.8 mW. The laser powers of the probing beam for ^{85}Rb and ^{87}Rb were 13 μW and 11 μW, respectively.

Figure 3 shows the absorption images of ^{85}Rb and ^{87}Rb atoms. The number of trapped ^{85}Rb is larger than that of trapped ^{87}Rb. The center positions of both atomic clouds are accordance in the 0.1-mm range. The radius of atomic cloud r_0, the atomic density n, and the number of atoms N observed without delay time are shown in Table 1.

The temperature of the atoms T can be estimated by the time-evolution of the radius of the atomic clouds $r(t)$, as follows.

$$r(t) = \sqrt{r_0^2 + \frac{2k_{\mathrm{B}}T}{m}t^2}, \tag{1}$$

where k_{B} is the Boltzmann constant and m is the mass of the atom. Figure 4 shows the radius of each isotope that was obtained after a certain delay time. The black lines represent the theoretical curve of Eq. (1) fitting to each data. The obtained temperature T of ^{85}Rb and ^{87}Rb atoms were $(2.1 \pm 0.4) \times 10^2$ μK and $(1.1 \pm 0.3) \times 10^2$ μK, respectively. To load atoms to the ODT efficiently, the temperature of the atoms should be reduced using polarization gradient cooling.

The shot-noise limits of the atomic magnetometers are limited by the number of atoms N.

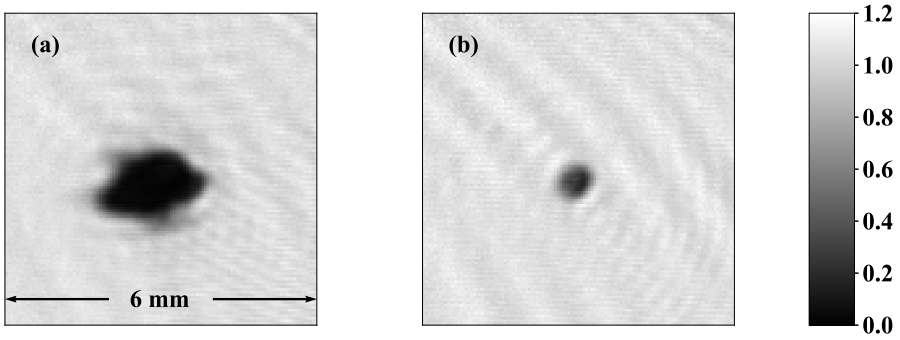

Figure 3. Absorption images of (a)^{85}Rb and (b)^{87}Rb atoms.

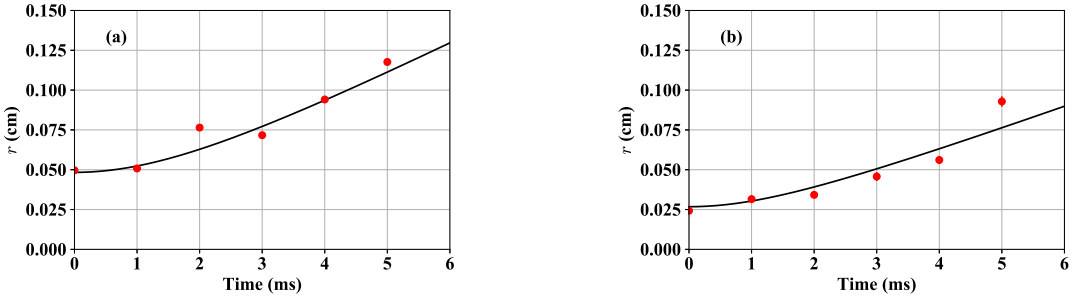

Figure 4. Time of flight of (a) ^{85}Rb and (b) ^{87}Rb atoms.

Table 1. Properties of trapped ^{85}Rb and ^{87}Rb atomic clouds.

	^{85}Rb	^{87}Rb
r_0 (cm)	$(4.8 \pm 0.4) \times 10^{-2}$	$(2.7 \pm 0.2) \times 10^{-2}$
n (cm^{-3})	$(4.7 \pm 0.3) \times 10^{10}$	$(5.3 \pm 0.3) \times 10^{10}$
N	$(3.2 \pm 0.3) \times 10^{6}$	$(4.2 \pm 0.4) \times 10^{5}$
T (μK)	$(2.1 \pm 0.4) \times 10^{2}$	$(1.1 \pm 0.3) \times 10^{2}$

If we ignore the VLS, the shot-noise limit of the magnetometer δB is estimated as follows.

$$\delta B = \frac{\hbar}{g_F \mu_B} \sqrt{\frac{\gamma}{N}} \tag{2}$$

Here, γ is the relaxation rate of the atomic spin coherence, g_F is the atomic g-factor, and μ_B is the Bohr magneton. Substituting the relaxation rate $\gamma = 1$ Hz and the number of atoms $N = 10^6$ into Eq. (2), δB for ^{85}Rb of 34 fT/$\sqrt{\text{Hz}}$ and ^{87}Rb of 23 fT/$\sqrt{\text{Hz}}$ are obtained. The loading efficiency from MOT-2 to the ODT in our ^{87}Rb apparatus is approximately 5×10^{-4}. To obtain these sensitivities, we need to increase the number of atoms trapped in the MOT to more than 10^8 and to achieve a high efficiency of loading to the ODT of approximately 10^{-2}.

4. Conclusion

The dual species co-magnetometer, which measures both the static magnetic field and the VLS, is crucial in the electron EDM search using laser-cooled Fr atoms. We reported the current development status of the dual-Rb-isotope co-magnetometer, especially on the dual-Rb-isotope MOT system using two individual lasers and EOMs. The number and temperature of the two isotopes were measured for ^{85}Rb and ^{87}Rb. Our results contribute toward realizing the dual species co-magnetometer. In the future, we will perform the electron EDM measurements using Fr and dual species co-magnetometer.

Acknowledgement

The authors thank U. Dammalapati, T. Hayamizu, H. Nagahama, N. Ozawa, and J. Tsutsumi for their helpful discussions. This work was supported by JSPS KAKENHI, Grant Nos. JP16J01466, JP26220705, JP16K17676, JP21104005, JP18K18762, and JP18K03663, the Tohoku University Division for International Advanced Research and Education, the SEI Group CSR Foundation, the Shimadzu Science Foundation, and the Futaba Electronics Memorial Foundation.

References

[1] Purcell E M and Ramsey N F 1950 *Phys. Rev.* **78** 807
[2] Fukuyama T 2012 *Int. J. Mod. Phys. A* **27** 1230015
[3] Pospelov M and Ritz A 2005 *Ann. Phys.* **318** 119
[4] Andreev V, *et. al.* 2018 *Nature* **562** 355
[5] Regan B C, Commins E D, Schmidt C J, and DeMille D 2002 *Phys. Rev. Lett.* **88** 071805
[6] Cairncross W B, Gresh D N, Grau M, Cossel K C, Roussy T S, Ni Y, Zhou Y, Ye J, and Cornell E A 2017 *Phys. Rev. Lett.* **119** 153001
[7] Hudson J J, Kara D M., Smallman I J, Sauer B E, Tarbutt M R, Hinds E A 2011 *Nature* **473** 493
[8] Mukherjee D, Sahoo B K, Nataraj H S, and Das B P 2009 *J. Phys. Chem. A* **113** 12549
[9] Byrnes T M R, Dzuba V A, Flambaum V V, and Murray D W 1999 *Phys. Rev. A* **59** 3082
[10] Harada K, *et. al.* 2016 *Appl. Opt.* **55** 1164
[11] Kawamura H, *et. al.* 2016 *Rev. Sci. Instrum.* **87** 02B921
[12] Inoue T, *et. al.* 2015 *Hyperfine Interact.* **231** 157
[13] Dammalapati U, *et. al.* 2017 *Proc. 12th Int. Conf. Low Energy Antiprot. Phys.* **18** 011046
[14] Harada K, *et. al.* 2016 *J. Phys. Conf. Ser.* **691** 012017
[15] Uchiyama A, *et. al.* 2018 *Rev. Sci. Instrum.* (to be published)